Gremlin-1: An endogenous BMP antagonist induces epithelial-mesenchymal transition and interferes with redifferentiation in fetal RPE cells with repeated wounds

Duo Li, Dongqing Yuan, Han Shen, Xiying Mao, Songtao Yuan, Qinghuai Liu

(These authors contributed equally to this work.)

Department of Ophthalmology, the First Affiliated Hospital of Nan Jing Medical University, Nanjing, China

Purpose: To investigate the role of Gremlin-1, which is an endogenous antagonist of the bone morphogenetic protein (BMP) signaling pathway, in inducing epithelium-mesenchymal transition (EMT) in fetal RPE cells after repeated wounds.
Methods: Subconfluent repetitive passages in fetal RPE cells were regarded as a model of repeated wounds. A phase contrast microscope was used to observe the morphology and pigment formation in cells. The expression of *GREM1* (Gene ID: 26585; OMIM 603054) and EMT- or RPE-related genes in cells was evaluated with quantitative PCR (qPCR). Recombinant human protein Gremlin-1 (0.1 μg/ml) was added every day to investigate the molecular effects of Gremlin-1 on fetal RPE cells. The cell migration rate was investigated using a cell wound scratch assay, and western blotting was used to analyze the representative proteins (P-cadherin, ZO-1, vimentin, Smad4, and phosphorylated-Smads). In addition, transfection of siRNA was used to explore the rescue effects on EMT cells through the downregulation of *GREM1*. Finally, LDN193189, which is a type of pan-inhibitor of BMP receptors, was used to verify whether complete blocking of the BMP pathway interferes with the redifferentiation in low-passage fetal cells, even if the cells were treated with transforming growth factor beta 1 (TGF-β) inhibitors.
Results: In fetal RPE cells, the expression of *GREM1* were gradually upregulated with repetitive passages, and at the same time, the function-specific genes in fetal RPE cells (*TJP1*, *PMEL*, *BEST1*, *RPE65*, and *MERTK*) were downregulated while the EMT-specific genes were upregulated. In addition, *GREM1* had a similar expression pattern as *SNAI1*, which is a key transcription factor to trigger EMT. Recombinant human Gremlin-1 promoted EMT with the upregulation of *SNAI1* and elevated the cell migration rate in a cell scratch assay, as well as decreased the expression of two key transcription factors of RPE embryonic development (*MITF* and *OTX2*) and the RPE marker, *RPE65*. Furthermore, the EMT marker, vimentin, and the TGF-β pathway downstream transcription factor phosphorylated-Smad2 (p-Smad2) increased, but the epithelial marker, ZO-1, was reduced. Additionally, Smad4, which plays a role as a Snail1 cooperator by binding Smad3, was also increased. In contrast, *GREM1* silencing increased the expression of *MITF* and *OTX2*, which means there was better redifferentiation in subconfluent fetal RPE cells, but it had little influence on p-Smad2 compared to the negative control group. Finally, by adding LDN193189, the BMP signaling pathway was blocked, and this block led to poor redifferentiation in low-passage cells, although the cells were treated with TGF-β inhibitors. In addition, as positive feedback to block the BMP pathway, *GREM1* was subsequently upregulated.
Conclusions: In fetal RPE cells, Gremlin-1 induces EMT and inhibits redifferentiation by promoting the TGF-β pathway and inhibiting the BMP pathway. *GREM1* silencing alleviates EMT and increases the redifferentiation of cells by relieving the blockade of the BMP pathway. However, *GREM1* silencing has no effects on the TGF-β pathway. Thus, Gremlin-1 may serve as a novel target to treat proliferative vitreoretinopathy (PVR) and inhibit subretinal fibrosis, which is a risk factor for influencing the therapeutic effects of anti-vascular endothelial growth factor (anti-VEGF) on neovascular age-related macular degeneration (nAMD).

RPE is the pigmented cell layer located between the neurosensory retina and the vascular choroid. Fibrosis in RPE causes diseases such as proliferative vitreoretinopathy (PVR) and neovascular age-related macular degeneration (nAMD) [1]. In fibrosis, epithelial-mesenchymal transition (EMT) has

been identified as a major driver, and in this process, epithelial cells such as RPE lose their polarity and tight junction. These changes result in an increase in migration and invasive properties [2]. In PVR, RPE cells become more invasive after EMT. These cells migrate into the vitreous cavity and form a contractile epiretinal membrane (ERM) that causes tractional retinal detachment [3]. In AMD, repetitive damage in RPE cells is generally considered to be the major pathogenesis that leads to the loss of central vision and choroidal

Correspondence to: Qinghuai Liu, Department of Ophthalmology, the First Affiliated Hospital of Nanjing Medical University, 300 Guangzhou Road, Nanjing, 210029, P.R. China; email: liuqh@njmu.edu.cn

neovascularization (CNV). Although intravitreal injection of anti-vascular endothelial growth factor (VEGF) medicine has become a standard therapeutic method for addressing CNV, subretinal fibrosis and formation of scars after injection threaten the therapeutic effect and result in unexpected visual acuity loss [4,5]. According to some studies, approximately half of the eyes after treatment could develop scars after 2 years, and in untreated CNV, scar formation is also an important morphological feature that influences the prognosis of disease [6,7]. EMT occurring in RPE is regarded as a major cause of this phenomenon [8].

The molecular mechanism of EMT is complex. Some transcription factors, such as Snail1, are conventionally known as keys to trigger the process, and some signaling pathways, such as the transforming growth factor beta 1 (TGF-β) pathway, are also important factors for promoting EMT [9]. In addition, bone morphogenetic protein (BMP), Notch, and the wingless (Wnt) pathways regulate this process [10]. These signaling pathways have extensive crosstalk, but the specific relationship in EMT is largely unknown [11]. Radekeet et al. confirmed that repetitively passaged RPE cells could induce EMT, and after treatment with A83–01, which is a TGF-β inhibitor, mesenchymal cells could be restored. However, when the cells were continuously passaged to passage 7, RPE cells still lost their functions and entered the mesenchymal state [12]. Therefore, a TGF-β inhibitor has great potential to prevent EMT of fetal RPE cells, but other factors that exist in the long run undermine the effectiveness of the inhibitor in an unknown way.

Gremlin-1 is one of the endogenous BMP antagonists that preferentially binds to BMP-2 or BMP-4 but secondarily binds to BMP-7 [13].In some research studies, BMP-4 and BMP-7 had inhibitory effects on EMT [14,15]. Therefore, Gremlin-1 likely promotes EMT by inhibiting BMP signaling. In some studies of pancreatitis and chronic kidney disease, Gremlin-1 was a key profibrotic factor for promoting fibrosis by inhibiting the BMP pathway and activating the TGF-β pathway. These studies also showed that *GREM1* (Gene ID: 26585; OMIM 603054) knockdown or knockout in cells or mice inhibit EMT [16,17]. In some cancers, such as mesothelioma, Gremlin-1 has been reported to promote cell migration and results in cancer cells that are more invasive by activating the TGF-β pathway and changing the extracellular matrix (ECM) [18]. Therefore, in this study, we investigated the effects of Gremlin-1 on inducing fetal RPE cells in the epithelial-mesenchymal transition and interfering with their redifferentiation.

METHODS

Fetal RPE cultures and treatments: RPE cells were isolated from three different aborted fetuses and cultured using a previously published protocol [19]. Plating density was 10,000 cells/cm^2, and the cultured medium was exchanged every 2 days. Cells that were needed to maintain differentiation were treated with SB431542 (Sigma, St. Louis, MO, 10 μM) every day. On day 32, cells were harvested by using trypsin and plated at 10,000 cells/cm^2 for routine serial passage. In addition, recombinant human Gremlin-1 (0.1 μg/ml, R&D, Shanghai, China) was added to the cells every day to explore the molecular functions of Gremlin-1 in RPE cells. The fetal RPE cells used in this study were obtained from the Center of Reproductive Medicine at the First Affiliated Hospital of Nanjing Medical University with informed consent and in accordance with the Declaration of Helsinki and the study adhered to the ARVO statement on human subjects.

An observation about the morphology and pigments of fetal RPE: The morphology of the cells cultured in vitro was observed with a phase contrast microscope (Nikon TS-100, Tokyo, Japan). And The pigments in cells were analyzed using bright-field micrographs [12].

Quantitative PCR (qPCR): Total RNA from cells was extracted using TRIzol (Invitrogen Life Technologies, Shanghai, China). cDNA was synthesized with a Revert Aid First Strand cDNA Synthesis Kit (Thermo, Shanghai, China). FastStart Universal SYBR Green Master (ROX; Roche, Basel, Switzerland) was used to amplify cDNA, and the StepOnePlus real-time PCR system (ABI, Carlsbad, CA) was used to detect the real-time change in cDNA. qPCR was conducted with the following protocol: 1 cycle of 95 °C for 3 min, followed by 45 cycles of 95 °C for 10 s, 58 °C for 20 s, 72 °C for 10 s. ΔΔCT was used to calculate the differences in relative gene expression, and the results represented the mRNA expression level. *ACTIN* (Gene ID:60; OMIM 102630) was used as an internal reference.

Cell scratch wound assay: Fetal RPE cells at passage 2 were grown to 100% confluency and divided into two groups (the control and Gremlin-1 groups). A marker pen was used to mark the edges of the scratches on the underside of the culture plates. A single scratch was made through the center of the cell sheets with a sterile pipette tip. The scratched areas were photographed immediately after wounding. After 2 days with treatment, the scratched areas were re-photographed using a phase contrast microscope, and the cell migration rate was assessed. Assays were performed in triplicate.

siRNA and transfection: *GREM1* siRNA (Silencer®Select, Ambion, Boston, MA) was used to knock down *GREM1*, and

negative control siRNA (Silencer™ FAM-labeled Negative Control No. 1 siRNA, Invitrogen, Boston, MA) was used as negative control. Lipofectamine 3000 (Invitrogen) was used to transfect siRNA into cells, and the method of transfection was conducted according to the reagent protocol (Invitrogen). After transfection, the cells were harvested on day 4 for measurement.

Western blotting: Fetal RPE cells were scraped off with cell scrapers and collected in a 1.5 ml centrifuge tube. Radioimmunoprecipitation assay (RIPA; Servicebio, Wuhan, China), which contained a protease inhibitor (Servicebio), was added and triturated with a pipette to ensure complete cell lysis in an ice bath for 30 min. The supernatant was collected after centrifuging for 10 min (20000 ×g, 4 °C). The protein samples were separated with sodium dodecyl sulfate–polyacrylamide gel electrophoresis (SDS–PAGE) gels and then transferred to the polyvinylidene difluoride (PVDF) membrane (Millipore, Shanghai, China). The membranes were incubated in the blocking buffer (5% nonfat dry milk or 5% bovine serum albumin [BSA] in 0.5% Tris-buffered saline/Tween 20 [TBST]) for 1 h at room temperature and hybridized with specific primary antibodies for P-cadherin (Abcam), Smad4, vimentin (Servicebio), phosphorylated-Smad2 (p-Smad2; BIOSS, Beijing, China), Smad1 (Ruiying Biology, Suzhou, China), and ZO-1 (Proteintech Group, Wuhan, China) at a dilution of 1:1,000 overnight at 4 °C. The membranes were washed three times before they were incubated with horseradish peroxidase (HRP)-conjugated secondary antibodies at an appropriate dilution (1:3,000) for 1 h at room temperature. The bands were visualized with an enhanced chemiluminescence (ECL) HRP substrate (Millipore) using a chemiluminescence imaging system (Syngene G:BOX Chemi HR16; Syngene, Frederick, MD). β-actin served as an internal reference.

Statistical analysis: All experiments were performed at least three times. The data are shown as the mean ± standard error of the mean (SEM) and were analyzed with GraphPad Prism 6 (GraphPad Software, San Diego, CA). Differences among the two groups were analyzed with a *t* test or a paired *t* test. One-way ANOVA (ANOVA) was used to analyze the samples that had more than two groups, and Dunnett's multiple comparisons test was performed with the control groups. A p value of less than 0.05 was considered statistically significant.

RESULTS

The expression of GREM1 was upregulated in the EMT of fetal RPE cells: Fetal RPE is one of the in vitro experimental models that resembles human RPE tissue more than ARPE-19. Generally, in early passages (from passage 1 to passage

3), most of the fetal RPE cells have a stable proliferation capacity and maintain some primal characteristic morphologies and functions, such as having a cobblestone-like appearance and pigments with abundant expression of some RPE function-specific genes, such as *MERTK* (Gene ID:10461, OMIM 604705), *BEST1* (Gene ID:7439,OMIM: 607854), *RPE65* (Gene ID:6121, OMIM 180069), *CDH1 (*Gene ID:999, OMIM 192090*)*, and *PMEL* (Gene ID: 6490, OMIM:155550). However, in this study, when cells were passaged to passage 4, the fetal RPE cells lost their characteristic shapes and pigments, and the cells gradually gained a fibroblast-like appearance (Figure 1A). The function-specific genes in fetal RPE cells decreased at passage 4 compared to the cells at passage 2 (Figure 1B). Moreover, passage 2 cells expressed more epithelial markers, especially *CDH1*, and the specific RPE epithelial marker P-cadherin also had more expression compared to the passage 4 cells (Figure 1C). However, compared to passage 2 cells, the EMT marker, *VIM* (Gene ID: 7431, OMIM: 193060), had higher expression in passage 4 cells (Figure 1D). In addition, the expression of *GREM1,* which encodes Gremlin-1, was statistically significantly upregulated in the passage 4 cells, which were in an EMT state (Figure 1E).

To investigate the expression level of *GREM1* in high passage cells when a TGF-β inhibitor prevented the rescue effects, fetal RPE cells were treated daily with SB431542 (10 μM). The cells treated with SB431542 had a more cobblestone-like appearance and pigments. However, when the cells were passaged to passage 11, the rescue effects of SB431542 disappeared because most of the cells became fibroblast-like, and the pigments were statistically significantly reduced (Figure 2A). Furthermore, the expression of RPE function-specific genes was decreased with repetitive passages (Figure 2B), and the expression of *GREM1* in SB431542-treated cells also had passage-related upregulation, especially in passage 11 cells (Figure 2C).

GREM1 and SNAI1 had a similar expression trend in the progress of the EMT: To explore the dynamic expression changes in *GREM1* in fetal RPE cells and EMT cells, the relation between *GREM1* and *SNAI1* (Gene ID: 6615 OMIM: 604238) was analyzed. Passage 4 cells, which were supposed to enter EMT, were seeded at 10,000 cells/cm^2 and were divided into two groups: one that was treated daily with SB431542 (the 10 μM SB431542 group), and the control group without any treatment (the control group). Cells were observed under microscopy and were harvested to evaluate the gene expression level and trend by qPCR on day 2, 5, 10, 15, and 30 after seeding. In the SB431542 group, the cells differentiated into RPE-like cells, while in the control group,
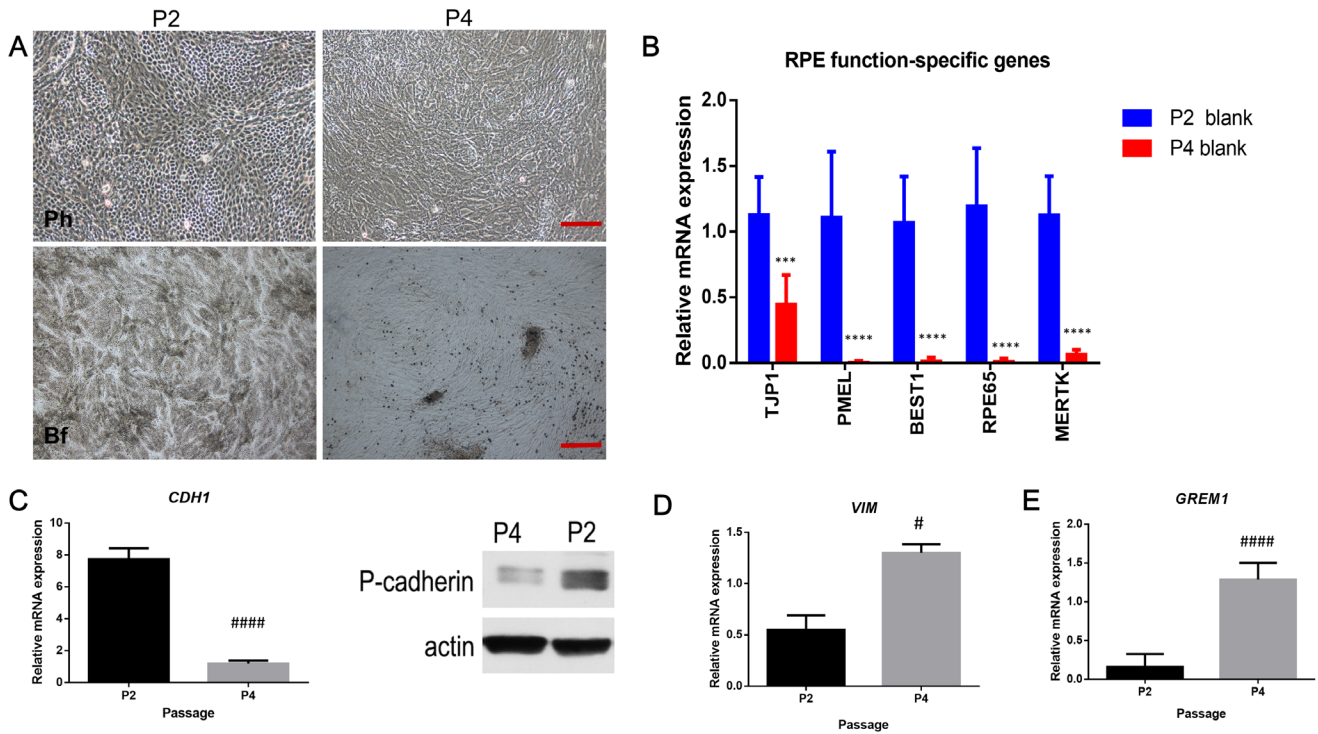
Figure 1. The expression of *GREM1* was upregulated in the epithelial-mesenchymal transition of fetal RPE cells. **A**: On day 32, passage 2 cells cultured without any treatment have a normal cobblestone-like appearance in phase contrast micrographs and more pigment in the bright-field micrographs, but passage 4 cells have a fibroblast-like shape and lost pigment. **B**: The related expression of RPE function-specific genes, such as *TJP1*, *PMEL*, *BEST1*, *RPE65*, and *MERTK*, decreased in passage 4 cells compared to passage cells. **C**: In passage 2 cells, *CDH1* had higher expression compared to passage 4 cells, and the western blotting results show that P-cadherin, which is a specific epithelial marker in RPE, is expressed more in passage 2 cells. **D**: *VIM*, which is a marker of epithelium-mesenchymal transition (EMT), has lower expression than passage 4 cells. **E**: The related expression of *GREM1* in passage 2 cells is lower than that of passage 4 cells. Scale bars: Ph: 100 μm, Bf: 500 μm. Data are shown as the mean ± standard error of mean (SEM), n=3, ****$p<0.0001$, ***$p<0.001$ versus P2 blank; ####$p<0.0001$, #$p<0.05$ versus P4 blank; Ph: Phase contrast; Bf: Bright-field *CDH1*: epithelial marker; *VIM*: EMT marker.

the cells gradually developed a fibroblast-like shape (Figure 3A). In addition, the expression of *GREM1* and *SNAI1* had a similar trend in both groups. In the control group, *SNAI1* was approximately upregulated along with the upregulation of *GREM1*. However, in the SB431542 group, *SNAI1* had low expression similar to *GREM1*. Meanwhile, *RPE65* was expressed in a gradually increasing manner while *GREM1* and *SNAI1* had low expression but maintained low expression when *GREM1* and *SNAI1* had high expression (Figure 3B).

Exogenous gremlin-1 induced EMT by upregulating SNAI1 and downregulating the expression of key transcription factors in fetal RPE cells: To explore the exact effects of Gremlin-1 fetal RPE cells, recombinant Gremlin-1 proteins (0.1 μg/ml, once per day) were added to passage 2 cells that were seeded at 10,000 cells/cm² until day 15. Obviously, the cells in the Gremlin-1 group appeared mesenchymal-like, but the cells in the control group appeared more cobblestone-like (Figure 4A). A cell wound scratch assay showed that the

cells in the Gremlin-1 group had a higher cell migration rate compared to the control group cells on the 2nd day after treatment (Figure 4B). Additionally, fetal RPE cells treated with recombinant Gremlin-1 proteins expressed more *SNAI1* and *VIM*; however, there was less *MITF* (Gene ID:4286 OMIM: 156845) and *OTX2* compared to the control group, and *RPE65* was also downregulated in the Gremlin-1 group cells (Figure 4C). Furthermore, in terms of the protein expression, ZO-1 had lower expression than the control group while vimentin had higher expression in the Gremlin-1 group (Figure 4D). Furthermore, a western blot showed that the active form of Smad2, p-Smad2, was enhanced, and at the same time, Smad4 also increased compared to the control group (Figure 4D).

GREM1 knockdown alleviated EMT and promoted redifferentiation in high passage fetal RPE cells by enhancing the BMP pathway: To investigate whether *GREM1* knockdown prevents EMT of fetal RPE cells, siRNA was transfected into
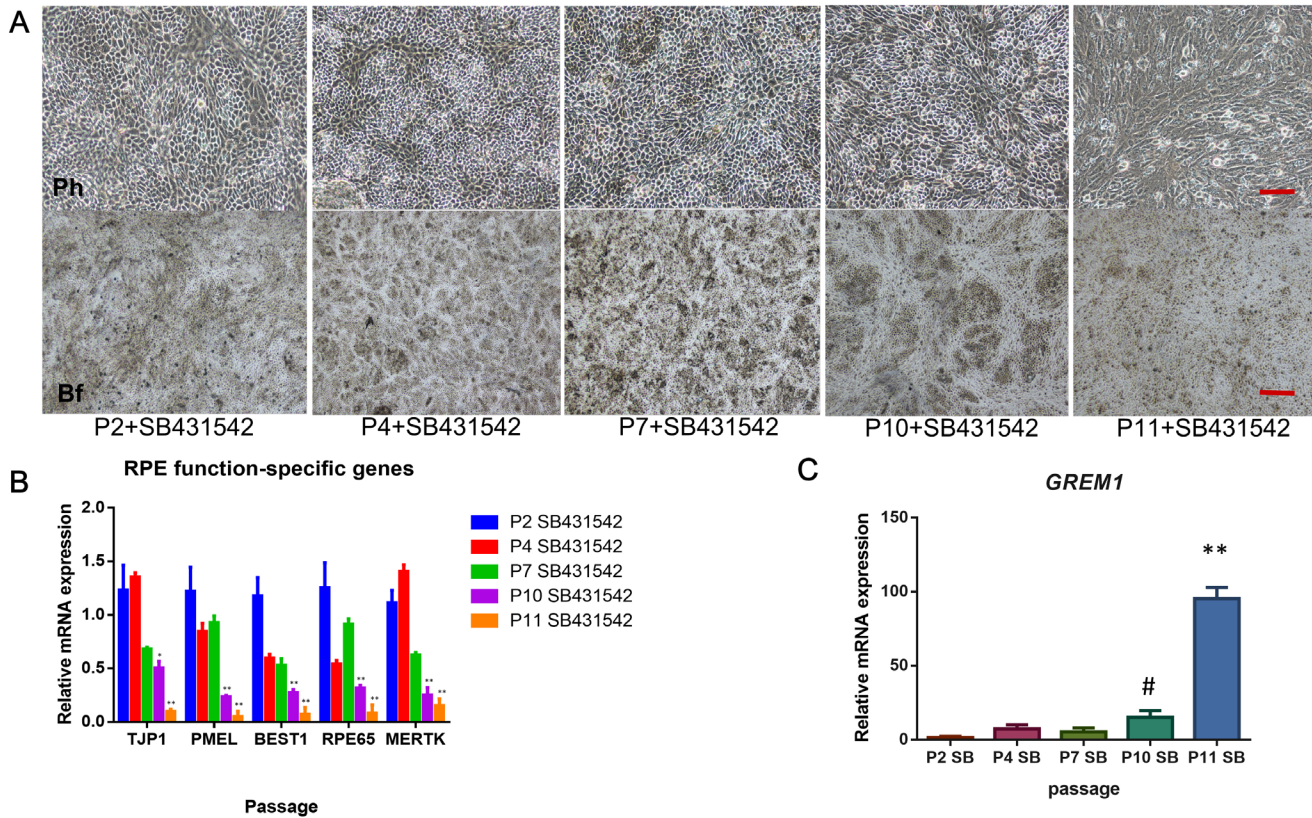
Figure 2. The expression of *GREM1* was upregulated in the epithelial-mesenchymal transition of fetal RPE cells. **A**: The phase contrast and bright-field micrographs show that fetal RPE cells treated with SB431542 every day maintained a cobblestone-like appearance and pigments until passage 11, and then they developed a fibroblast-like appearance and lost their pigment. **B**: When cells are repetitively passaged, the expression of RPE function-specific genes shows a relatively declining trend, and passage 11 cells have the lowest expression levels. **C**: The expression of *GREM1* is increased gradually with repetitive passages, and passage 11 cells have the highest expression compared to the other passages. Scale bar: Ph: 100 μm, Bf: 500 μm. Data are shown as the mean ± standard error of mean (SEM), n=3, **p<0.0001, *p<0.001, #p<0.05 versus P2 SB431542. Ph: Phase contrast; Bf: Bright-field SB: SB431542.

cells, and the transfection efficiency was confirmed with qPCR (Figure 5A). On the 4th day after transfection, the si*GREM1* group cells appeared to have a more cobblestone-like shape, but all of the negative control (NC) group cells maintained a fibroblast-like shape (Figure 5B). Meanwhile, in the si*GREM1* group cells, the expression level of *MITF*, *OTX2*, and *RPE65* increased and that of *VIM* decreased. However, *SNAI1* had no statistically significant change compared to the NC group cells (Figure 5C). For the changes in the representative protein expression after transfection, ZO-1 and p-Smad1 increased, vimentin was reduced, and p-Smad2 between the si*GREM1* and NC group cells had no statistically significant differences (Figure 5D).

Completely blocking the BMP pathway inhibited redifferentiation in low passage fetal RPE cells and upregulated GREM1: BMPs play an important role in the embryonic development of RPE, and they have some effects on inhibiting EMT [14,15]. Although Gremlin-1 is one of the endogenous BMP antagonists that binds BMPs and is upregulated in mesenchymal RPE, binding some kinds of BMPs did not provide abundant evidence to prove that completely blocking the BMP pathway would inhibit mostly sub-confluent low passage fetal RPE cells from redifferentiating into fetal RPE cells. Therefore, LDN193189 was used as a pan-inhibitor to verify whether inhibition of the BMP pathway interferes with redifferentiation. LDN193189 is a selective chemical inhibitor of BMP type I receptor kinases, which interrupts the phosphorylation activity of BMP type I receptors ALK2 and ALK3 (IC_{50}=5 nM and 30 nM, respectively). Therefore, the molecular concentration was kept to 100 nM to ensure the suppressive efficiency of the BMP pathway and to avert other redundant concentration-related effects, such as inhibition of TGF-β type I receptors (ALK4, ALK5, and ALK7, IC_{50}≥500 nM). Passage 2 cells were divided into four groups: the
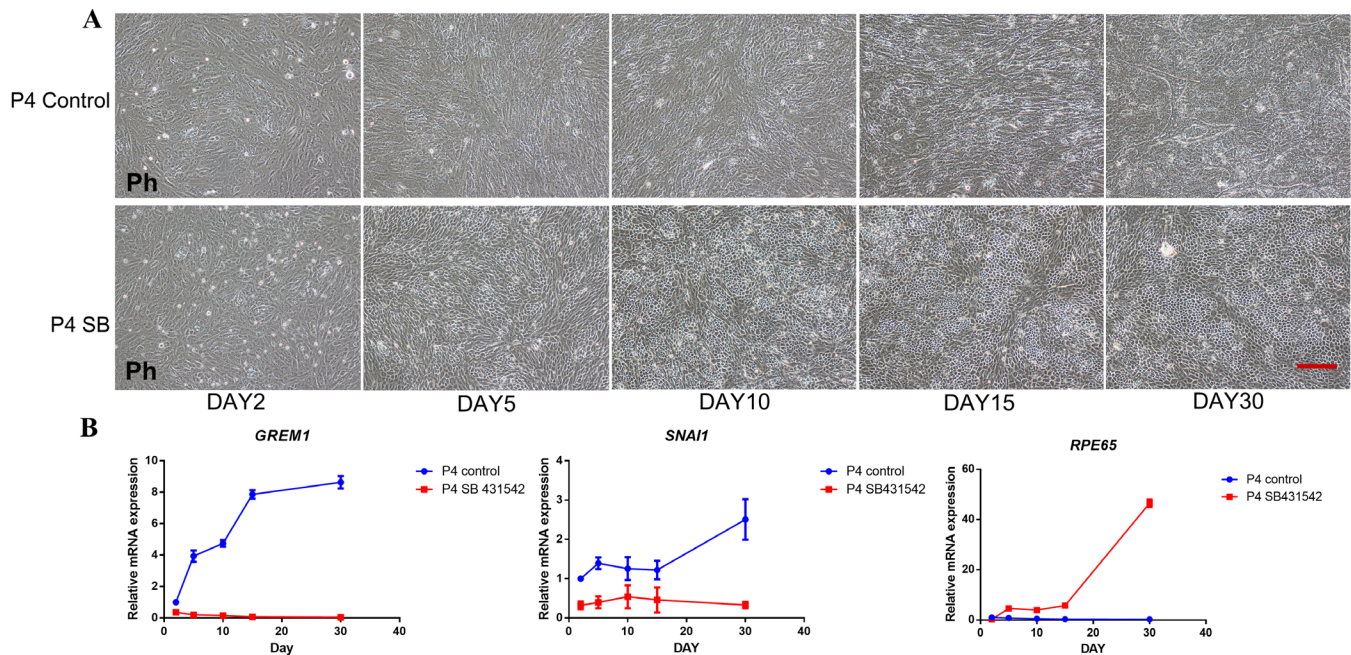
Figure 3. *GREM1* and *SNAI1* had a similar expression trend in the progress of the epithelial-mesenchymal transition. **A**: The phase contrast micrographs show that the SB431542 group cells on day 2, 5, 10, 15, and 30 gradually develop the common morphology of fetal RPE cells, but the control group cells lose the appearance of fetal RPE cells and gain mesenchymal-like appearances. **B**: The quantitative PCR (qPCR) results show that the relation between *GREM1* and *SNAI1* in cells that were harvested on day 2, 5, 10, 15, and 30 had a similar trend. In the control group cells, *GREM1* is upregulated gradually in the same manner as *SNAI1*, but *RPE65* retains lower expression. In the SB431542 group cells, *GREM1* and *SNAI1* maintain lower expression while *RPE65* is upregulated gradually. Scale bar: 500 µm. Data are shown as the mean ± standard error of mean (SEM), n=3. Ph: Phase contrast; SB: SB431542.

control, SB431542 (SB group), SB431542+LDN193189 (S+L group), and LDN193189 (LDN group) groups. After treatment, cells in the LDN and S+L groups had a poor appearance with abnormal shapes and lacked pigment compared to the control group and SB group cells. The control group cells and the SB group cells had no statistically significant differences in their morphology (Figure 6A). In addition, RPE function-specific genes in the LDN group and S+L group cells had much lower expression than the other two groups (Figure 6B), and *GREM1* was upregulated after LDN193189 was used, especially in the LDN group (Figure 6C).

DISCUSSION

EMT is one of the most important pathological changes in RPE wound responses. EMT is not only the key process in the pathogenesis of PVR but also causes fibrosis in the subretinal space that decreases the therapeutic effects of anti-VEGF on retinal neovascular diseases, such as CNV. Thus, the need to inhibit EMT for treating retinal fibrosis is extremely urgent. Although TGF-β inhibitors can rescue mesenchymal RPE, they always have a smaller effect on cells with repetitive

wounds, such as cells that are repetitively passaged in vitro. Therefore, other factors must promote EMT.

Gremlin-1 is an endogenous BMP antagonist. Gremlin-1 serves as a negative regulator in the self-feedback system in the BMP signaling pathway and interacts with neighbor cells or itself through paracrine or autocrine mechanisms [20]. Gremlin-1 predominantly binds to BMP-2 and BMP-4, and interferes with their binding to receptors. In this study, mesenchymal RPE cells expressed more *GREM1*, although they were treated with SB431542 to inhibit EMT after several passages. The expression process of *GREM1* in the EMT cells showed an approximately similar trend to *SNAI1*; however, *GREM1* was already shown to be upregulated before *SNAI1* expression. According to studies in other diseases, Gremlin-1 promotes EMT in renal fibrosis and chronic pancreatitis, as well as enhances cancer cell invasiveness, such as mesothelioma cells. The results of these studies indicated that Gremlin-1 could promote *SNAI1* expression, but the exact mechanism of this promotion is unknown. The same results were also verified in the present study, and the fetal RPE cells treated with recombinant Gremlin-1 protein expressed
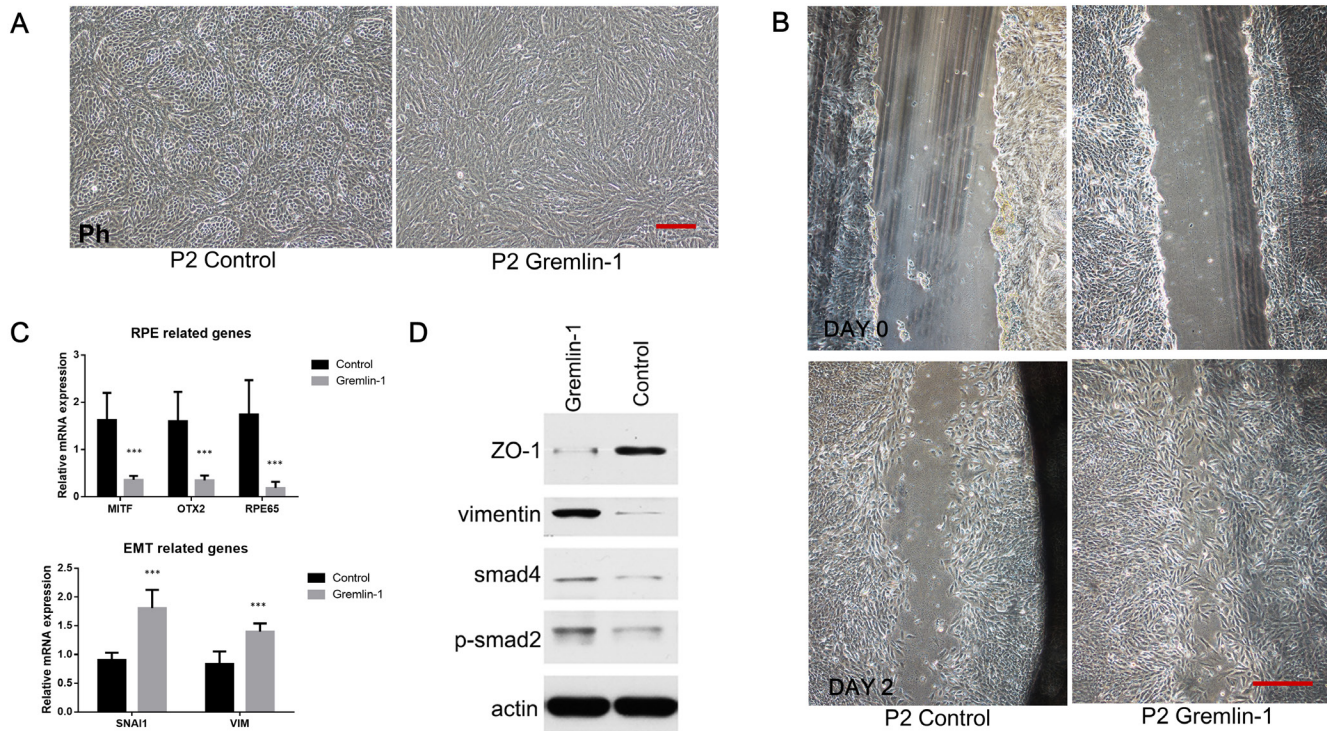
Figure 4. Exogenous Gremlin-1 induced EMT by upregulating *SNAI1* and downregulating the expression of key transcription factors in fetal RPE cells. **A**: The phase contrast micrographs show that passage 2 cells treated with recombinant human Gremlin-1 develop a mesenchymal-like appearance compared with the control group cells. **B**: Cell scratch wound assays show that the cells with the Gremlin-1 treatment have more cell migration after 2 days. **C**: The quantitative PCR (qPCR) results show that the EMT-related genes, *SNAI1* and *VIM*, are upregulated after Gremlin-1 treatment, while the RPE-related genes (*MITF*, *OTX2*, and *RPE65*) are downregulated. **D**: The western blotting results show that Gremlin-1 reduces ZO-1 expression and increases vimentin, and after Gremlin-1 treatment, p-Smad2 and Smad4 are upregulated. Actin serves as an internal reference in the western blots. Scale bar: Ph: 100 μm. Data are shown as the mean ± standard error of mean (SEM), n=3, ***$p < 0.001$ versus control. Ph: Phase contrast; p-Smad2: phosphorylated-Smad2.

more *SNAI1*. Therefore, it is not clear whether Gremlin-1 is one of the determining factors for *SNAI1* expression, but it is likely one of the stimulators. Therefore, to detect the real effects on cells, recombinant human Gremlin-1 was used, and it obviously facilitated RPE cell migration, which is one of the mechanisms underlying retinal detachment in PVR. According to the western blotting results, Gremlin-1 not only inhibited the BMP pathway but also promoted the TGF-β pathway because of an increase in p-Smad2, which is an activated transcription factor downstream of the TGF-β pathway. At the same time, Smad4, which binds Smad3 and cooperates with Snail1, was also increased [9]. The TGF-β pathway is one of the most important pathways that triggers EMT, but in some ways, the BMP pathway plays a negative role in the occurrence of EMT [15]. Therefore, Gremlin-1 exacerbates EMT by inhibiting BMP signaling and promotes TGF-β signaling to induce EMT.

In the embryonic development of eyes, BMPs secreted by the surface ectoderm can specify RPE development in chick embryos. In the optic cup without a surface ectoderm, exogenous BMPs can rescue the function of these cells and initiate *MITF* expression so that it triggers embryonic development of RPE [21,22]. Generally, low passage fetal cells express *MITF* and *OTX2* and regain a hexagon shape and pigments [23,24]. However, in the present study, exogenous Gremlin-1 downregulated the expression of *MITF* and *OTX2* in low passage cells, which indicates that blockade of the BMP pathway leads to poor differentiation in fetal RPE cells. In contrast, *GREM1* knockdown by transfecting siRNA relieved the downregulation effects of Gremlin-1 on *MITF* and *OTX2* and rescued high passage mesenchymal RPE cells. However, *SNAI1* maintained a similar expression level compared with its expression in the NC group cells, but *VIM* decreased in a novel way. The possible reasons for this phenomenon are that p-Smad1 increased, but p-Smad2 had no statistically significant change, and these results indicate
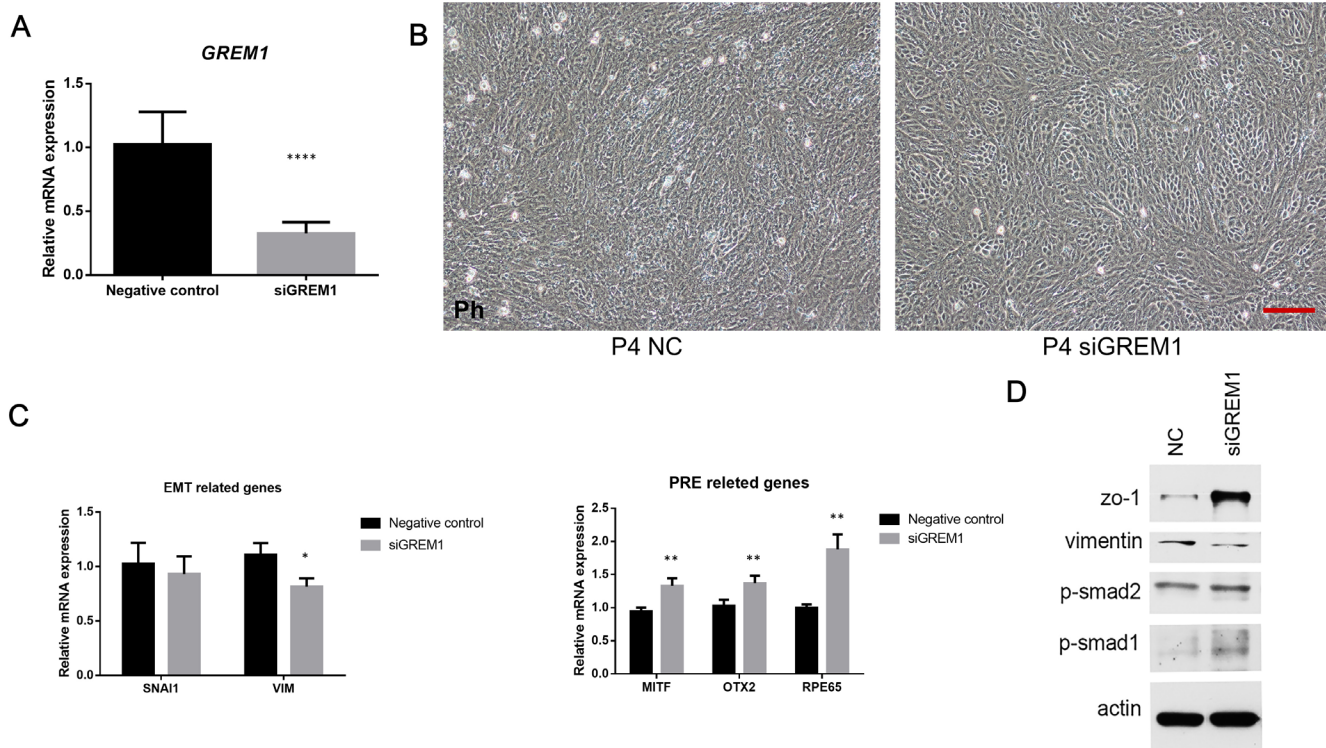
Figure 5. *GREM1* knockdown alleviated EMT and promoted redifferentiation in high passage fetal RPE cells by enhancing the BMP pathway. **A**: The quantitative PCR (qPCR) results show that the *GREM1* knockdown makes *GREM1* downregulate efficiently. **B**: On day 4 after transfection, some si*GREM1* group cells appear to have a relatively normal cobblestone-like shape compared to the NC group cells and an appearance less like epithelium-mesenchymal transition (EMT). **C**: The qPCR results show that after transfection, *SNAI1* had no statistically significant difference, but *VIM* is reduced, and the RPE-related genes, such as *MITF*, *OTX2*, and *RPE65* are upregulated in the si*GREM1* group cells compared to the NC group cells. **D**: The western blotting results show that in the si*GREM1* group cells, ZO-1 and p-Smad1 are increased, but vimentin is decreased compared to the NC group cells. However, p-Smad2 has no statistically significant differences between the two groups. Actin serves as an internal reference in the western blots. Scale bar: 100 μm. Data are shown as the mean ± standard error of mean (SEM), n=3, **p<0.01 *p<0.05 versus NC groups. Ph: Phase contrast micrograph; si*GREM1*: *GREM1* knockdown by siRNA group; NC group: Negative group. p-Smad2: phosphorylated-Smad2; p-Smad1: phosphorylated-Smad1.

that *GREM1* knockdown can alleviate the suppression of the BMP signaling pathway but may lack an ability to inhibit the TGF-β pathway. Therefore, although stable TGF-β signals induce continuous *SNAI1* expression, *GREM1* knockdown facilitates activation of the BMP pathway to induce RPE differentiation by upregulating *MITF* and *OTX2*. These results counteract the effects of TGF-β [9]. In addition, although some cells were treated with SB431542, LDN193189 (as an inhibitor of the BMP type I receptor) still interfered with the redifferentiation in low passage fetal RPE cells, and the expression of *GREM1* was simultaneously increased. These results reveal that complete inhibition of ALK2 and ALK3 can promote EMT and interrupt fetal RPE cells redifferentiation, and the upregulation of *GREM1* further induces EMT as positive feedback. The results also reveal that the BMP pathway is necessary for redifferentiation in fetal RPE cells, but Gremlin-1 has a similar negative effect as LDN193189. In

contrast, inhibiting TGF-β with SB431542 had no influence on low passage cells.

Until recently, there had been no specific chemical molecule to inhibit Gremlin-1; therefore, there has been no opportunity to confirm whether persistently inhibiting Gremlin-1 restores mesenchymal RPE instead of transient downregulation using siRNA. Meanwhile, stable transfection should also be used to make long-term observations. However, the transient transfection results reveal that there is a potential chance to inhibit EMT when TGF-β inhibitors lose their effects. In addition, Gremlin-1 has other novel biologic functions. In bones and intestines, the expression of *GREM1* defines osteochondral reticular (OCR) stem cells and intestinal reticular stem cells (iRSCs) [25]. Researchers have also identified that Gremlin-1 is a proangiogenic regulator like VEGF that binds vascular endothelial factor receptor 2

(VEGFR2) and can increase angiogenesis in vitro or in vivo [16] [26]. The results suggest that Gremlin-1 may be not only a promoter of fibrosis but also an inducer of neovascular disease in the retina. Therefore, Gremlin-1 is likely to be a potential therapeutic target for some intraocular diseases, like PVR, proliferative diabetic retinopathy (PDR), and neovascular AMD, through antifibrosis and anti-neovascularization mechanisms.

Gremlin-1 is not the only endogenous BMP inhibitor. Several endogenous inhibitors, such as Noggin and chordin (chordin-like 1 and chordin-like 2), also have the ability to block the BMP signaling pathway, but the relation and exact functions of these factors for EMT are unknown [14]. However, as a hypothesis, these factors could have some

regulating effects on RPE cells in embryonic development, differentiation, and EMT. This possibility needs to be studied further.
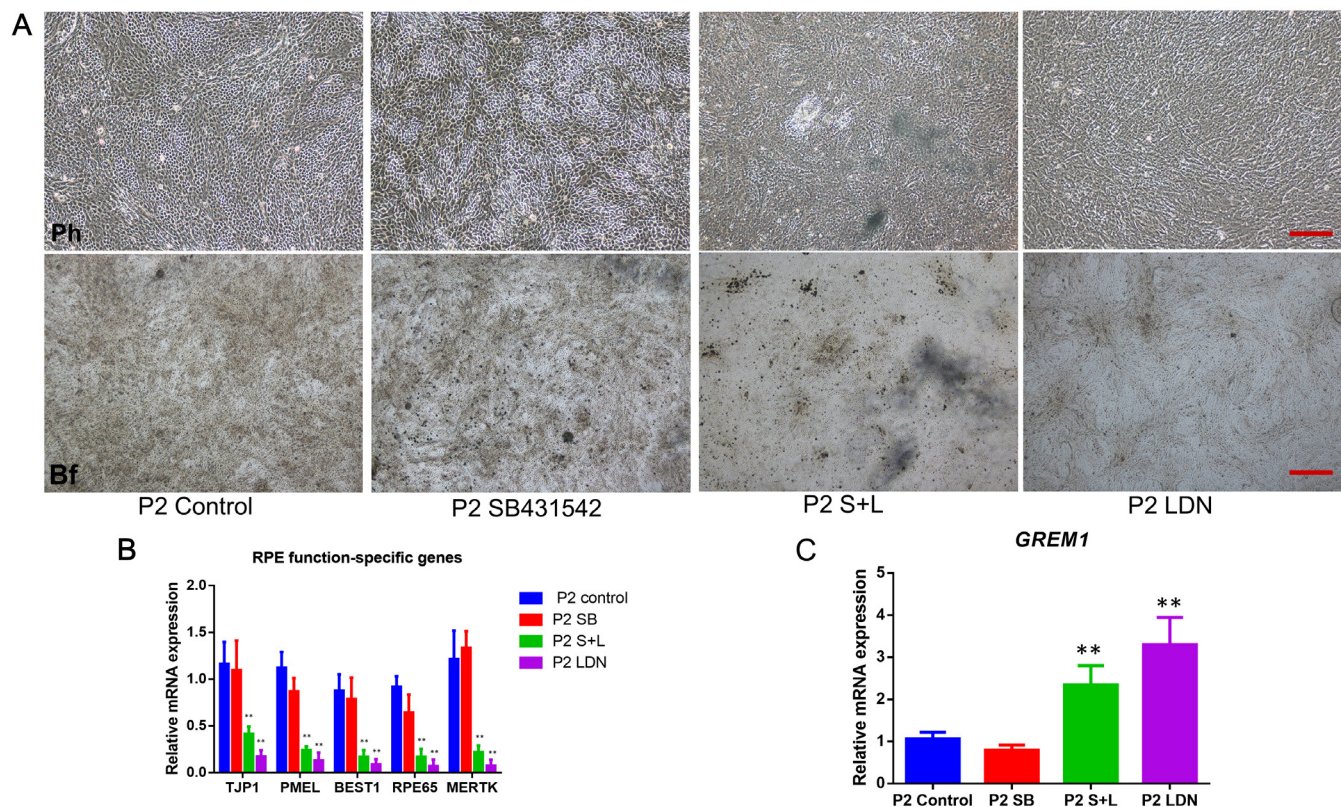
ACKNOWLEDGMENTS

Figure 6. Completely blocking the BMP pathway inhibited redifferentiation in low passage fetal RPE cells and upregulated *GREM1* **A**: Four groups: the control group, SB group, S+L group, and LDN group. After treatment, the phase contrast micrographs demonstrate that the cells treated with dual pathway inhibitors or LDN193189 had poor differentiation, but other groups without BMP inhibitors grew well and are pigmented. **B**: The quantitative PCR (qPCR) results show that the expression of RPE function-specific genes in the S+L group and LDN group cells is much lower than cells in other groups, but the control group cells and the SB group cells had no statistically significant differences. **C**: The expression of *GREM1* in the S+L group and LDN group cells is upregulated compared to that of the other groups without the BMP inhibitor treatment. Scale bar: Ph: 100 μm; Bf: 500 μm. Data are shown as the mean ± standard error of mean (SEM), n=3, **p<0.01 versus P2 control group. Ph: Phase contrast; Bf: Bright-field; SB group: SB431542 group; S+L group: SB431542+LDN193189 group; LDN group: LDN193189 group.

REFERENCES

1. Friedlander M. Fibrosis and diseases of the eye. J Clin Invest 2007; 117:576-86. J.

2. Nieto MA, Huang RYJ, Jackson R, Thiery JP. EMT: 2016 Cell 2016; 166:21-45. J.

3. Tamiya S, Kaplan HJ. Role of epithelial–mesenchymal transition in proliferative vitreoretinopathy Exp Eye Res 2016; 142: :26-31. J.

4. Nowak JZ. AMD–the retinal disease with an unprecised etiopathogenesis: in search of effective therapeutics. Acta Pol Pharm 2014; 71:900-16. J.

5. Salomon Y. Cohen, Hassiba Oubraham, Joel Uzzan, Lise Dubois, Ramin Tadayoni. Causes of unsuccessful ranibizumab treatment in exudative age-related macular degeneration in clinical settings. Retina 2012; 32:1480-85-.

6. Daniel E, Cynthia A. Toth, Juan E Grunwald, Glenn J Jaffe, Daniel F Martin, Stuart L Fine, Jiayan Huang, Guishuang Ying, Stephanie A Hagstrom, Katrina P Winter, Maureen G Maguire. Risk of Scar in the Comparison of Age-related Macular Degeneration Treatments Trials Ophthalmology 2014; 121:656-66. J.

7. Daniel E, Pan W, Ying G, Benjamin J. Kim, Juan E Grunwald, Frederick L Ferris, Glenn J Jaffe, Cynthia A Toth, Daniel F Martin, Stuart L Fine, Maureen G Maguire. Development and Course of Scars in the Comparison of Age-related Macular Degeneration Treatments Trials Ophthalmology 2018; 125:1037-1046. .

8. Ishikawa K, Kannan R, Hinton DR. Molecular mechanisms of subretinal fibrosis in age-related macular degeneration Exp Eye Res 2015; 142:19-25. J.

9. Lamouille S, Xu J, Derynck R. Molecular mechanisms of epithelial–mesenchymal transition Nat Rev Mol Cell Biol 2014; 15:178-96. J.

10. Gonzalez DM, Medici D. Signaling mechanisms of the epithelial-mesenchymal transition Sci Signal 2014; 7:re8-J.

11. Guo X, Wang X. Signaling cross-talk between TGF-β/BMP and other pathways Cell Res 2009; 19:71-88. J.

12. Monte J. Radeke, Carolyn M Radeke, Yinghsuan Shih, Jane Hu, Dean Bok, Lincoln V Johnson, Peter J Coffey. Restoration of mesenchymal retinal pigmented epithelial cells by TGFβ pathway inhibitors: implications for age-related macular degeneration Genome Med 2015; 7:58-58. J.

13. Derek P. Brazil, Rachel H Church, Satnam Surae, Catherine Godson, Finian Martin. BMP signalling: agony and antagony in the family Trends Cell Biol 2015; 25:249-64. J.

14. Zeisberg M, Shah A, Kalluri R. Bone Morphogenic Protein-7 Induces Mesenchymal to Epithelial Transition in Adult Renal Fibroblasts and Facilitates Regeneration of Injured Kidney J Biol Chem 2005; 280:8094-100. J.

15. Yao H, Li H, Yang S, Li M, Zhao C, Zhang J, Xu G, Wang F. Inhibitory Effect of Bone Morphogenetic Protein 4 in Retinal Pigment Epithelial-Mesenchymal Transition. Sci Rep 2016; 6:J.

16. Staloch D, Gao X, Liu K, Xu M, Feng X, Judith F Aronson MF, George H. Greeley, Cristiana Rastellini, Celia Chao, Mark R Hellmich, Yanna Cao, Tien C Ko. Gremlin is a key pro-fibrogenic factor in chronic pancreatitis J Mol Med 2015; 93:1085-93. 32182.

17. Rodriguesdiez R, Lavoz C, Carvajal G, Rayegomateos S, Diez RR, Ortiz A, Egido J, Mezzano S, Ruizortega M. Gremlin is a downstream profibrotic mediator of transforming growth factor-beta in cultured renal cells Nephron, Exp Nephrol 2012; 122:62-J.

18. Yin M. Mira Tissari, Jenni Tamminen, Irene Ylivinkka, Mikko Ronty, Pernilla Von Nandelstadh, Kaisa Lehti, Marko Hyytiainen, Marjukka Myllarniemi, Katri Koli. Gremlin-1 is a key regulator of the invasive cell phenotype in mesothelioma Oncotarget 2017; 8:98280-97. J.

19. Gamm D. J Nicholas Melvan, R L Shearer, I Pinilla, Grzegorz Sabat, Clive N Svendsen, Lynda S Wright. A Novel Serum-Free Method for Culturing Human Prenatal Retinal Pigment Epithelial Cells Invest Ophthalmol Vis Sci 2008; 49:788-99. J.

20. Scheel C, Eaton EN, Li S, Christine L. Chaffer, Ferenc Reinhardt, Kong Jie Kah, George W Bell, Wenjun Guo, Jeffrey S Rubin, Andrea L Richardson, Robert A Weinberg. Paracrine and autocrine signals induce and maintain mesenchymal and stem cell states in the breast. Cell 2011; 145:926-40. J.

21. Muller F, Rohrer H, Vogelhopker A. Bone morphogenetic proteins specify the retinal pigment epithelium in the chick embryo Development 2007; 134:3483-93. J.

22. Steinfeld J, Steinfeld I, Coronato N, Hampel M, Paul G. Layer, Masasuke Araki, Astrid Vogelhopker. RPE specification in the chick is mediated by surface ectoderm-derived BMP and Wnt signalling Development 2013; 140:4959-69. J.

23. Singh R. M Joseph Phillips, David Kuai, Jackelyn Meyer, Jessica M Martin, Molly A Smith, Enio T Perez, Wei Shen, Kyle Wallace, Elizabeth E Capowski, Lynda S Wright, David M Gamm. Functional Analysis of Serially Expanded Human iPS Cell-Derived RPE Cultures Invest Ophthalmol Vis Sci 2013; 54:6767-78. J.

24. Shih Y, Monte J. Radeke, Carolyn M Radeke, Peter J Coffey. Restoration of Mesenchymal RPE by Transcription Factor-Mediated Reprogramming. Invest Ophthalmol Vis Sci 2017; 58:430-430. J.

25. Daniel L. Worthley, Michael Churchill, Jocelyn T Compton, Yagnesh Tailor, Meenakshi Rao, Yiling Si, Daniel E Levin, Matthew G Schwartz, Aysu Uygur, Yoku Hayakawa, Stefanie Gross, Bernhard W Renz, Wanda Setlik, Ashley N Martinez, Xiaowei Chen, Saqib Nizami, Heon Goo Lee, H Paco Kang, Jonmichael Caldwell, Samuel Asfaha, C Benedikt Westphalen, Trevor A Graham, Guangchun Jin, Karan Nagar, Hongshan Wang, Mazen A Kheirbek, Alka Kolhe, Jared Carpenter, Mark A Glaire, Abhinav Nair, Simon Renders, Nicholas A Manieri, Sureshkumar Muthupalani, James G Fox, Maximilian Reichert, Andrew S Giraud, Robert F Schwabe, Jeanphillipe Pradere, Katherine D Walton, Ajay Prakash, Deborah L Gumucio, Anil K Rustgi, Thaddeus S Stappenbeck, Richard A Friedman, Michael D Gershon,

Peter A Sims, Tracy C Grikscheit, Francis Y Lee, Gerard Karsenty, Siddhartha Mukherjee, Timothy C Wang. Gremlin 1 Identifies a Skeletal Stem Cell with Bone, Cartilage, and Reticular Stromal Potential Cell 2015; 160:269-84. J.

26. Mitola S, Ravelli C, Moroni E, Salvi V, Leali D, Ballmerhofer K, Zammataro L, Presta M. Gremlin is a novel agonist of the major proangiogenic receptor VEGFR2. Blood 2010; 116:3677-80. J.